Effect of Temperature on the Oil Stability Index (OSI) of Biodiesel

Robert O. Dunn*

Food and Industrial Oils Research, United States Department of Agriculture (USDA), Agriculture Research Service, National Center for Agricultural Utilization Research, Peoria, Illinois 61604

Received July 16, 2007. Revised Manuscript Received October 23, 2007

Biodiesel, an alternative fuel derived from lipid feedstocks, such as vegetable oil or animal fat, is mainly composed of saturated and unsaturated fatty acid alkyl esters. Fuel suppliers, terminal operators, and users are becoming more concerned with monitoring and maintaining good biodiesel fuel quality with respect to oxidative degradation during storage. The oil stability index (OSI), a parameter that measures the relative oxidative stability of fatty materials, is typically measured isothermally at elevated temperatures to accelerate oxidation. The present work investigates the effects of block temperature (T) on the OSI of biodiesel from soybean oil fatty acid methyl esters (SME) and used cooking oil fatty acid methyl esters (UCOME). Results were compared to those for pure methyl oleate (MO). An increasing temperature accelerated the oxidation reaction causing a decrease in OSI. Response factors (RF) determined with MO as the reference methyl ester showed little variation with respect to the temperature ranges studied. At constant T, SME yielded lower OSI values than either UCOME or MO. However, despite having comparable iodine values, UCOME yielded a significantly higher OSI than MO. Two mathematical models for determining OSI as a function of T demonstrated linear correlations for all three methyl esters. Results from the second model, ln(OSI) versus T^{-1}, were employed to calculate the activation energy (E_a) of first-order oxidation reactions. Although both models exhibited relatively small deviations between calculated and measured OSI values, the models were not reliable at temperatures below 50 °C.

Introduction

Biodiesel is defined as fatty acid monoalkyl esters derived from the transesterification of agricultural lipids such as vegetable oil, used cooking oil, waste greases, or animal fat. In the United States, the most common forms are fatty acid methyl esters (FAME) and ethyl esters. Biodiesel is ideal as an alternative fuel or fuel extender for combustion in compression-ignition (diesel) engines in many applications, including trucks and automobiles, farm vehicles, locomotives, aircrafts, stationary power generators, boilers, and heaters.

Several recent reviews[1–3] have outlined the many technical merits of biodiesel. Biodiesel is a renewable fuel that can be made from local feedstocks, is environmentally innocuous because of its low toxicity and propensity to biodegrade, and is relatively safe to store and handle because of a high flash point. Biodiesel has gross heat of combustion, specific gravity, and kinematic viscosity comparable to conventional diesel (petrodiesel). It blends well with petrodiesel and enhances the cetane number, which decreases ignition delay times. Biodiesel is known to enhance lubricity and antiwear characteristics when blended with low-sulfur petrodiesel.[3,4] It was reported that biodiesel returns more than 3 times the energy required to produce it and has a net negative carbon dioxide balance.[5] A comprehensive review by the U.S. Environmental Protection Agency[6] showed that biodiesel reduces regulated exhaust emissions including hydrocarbons, carbon monoxide, and particulate matter when blended with petrodiesel. The degree in which emissions are reduced was approximately linear with respect to the blend ratio. Biodiesel similarly reduces smoke opacity, sulfur dioxide, and polycyclic aromatic hydrocarbon emissions.[1–3] Its main disadvantages include poor long-term storage stability characteristics, poor cold weather performance, and causing slight increases in emissions of nitrogen oxides compared to petrodiesel.

Storage stability of a liquid fuel is defined by its ability to resist physical and chemical changes brought about by interactions with its environment.[7] Stability may be affected by interactions with contaminants, light, factors that cause sediment formation, changes in color, and other changes that reduce cleanliness of the fuel.[8] Mechanisms that degrade fuel properties during storage include oxidation or autoxidation from contact with ambient air, thermal-oxidative decomposition from excess heat, hydrolysis from contact with water or moisture in tanks

* To whom correspondence should be addressed. Telephone: 309-681-6101. Fax: 309-681-6340. E-mail: Robert.Dunn@ars.usda.gov.

(1) Knothe, G.; Dunn, R. O. *Industrial Uses of Vegetable Oils*; Erhan, S. Z., Ed.; AOCS Press: Champaign, IL, 2005; pp 42–89.

(2) Knothe, G.; Dunn, R. O. *Oleochemical Manufacture and Applications*; Gunstone, F. D., Hamilton, R. J., Eds.; Sheffield Academic: Sheffield, U.K., 2001; pp 106–163.

(3) Graboski, M. S.; McCormick, R. L. *Prog. Energy Combust. Sci.* **1998**, *24*, 125–164.

(4) Van Gerpen, J. H.; Soylu, S.; Tat, M. E. Evaluation of the lubricity of soybean oil-based additives in diesel fuels. In Proceedings of the Annual Meeting of the ASAE, American Society of Agricultural Engineers, St. Joseph, MI, 1999; paper number 996314.

(5) Sheehan, J.; Camobreco, V.; Duffield, J.; Graboski, M.; Shapouri, H. Life cycle inventory of biodiesel and petroleum diesel for use in an urban bus. Final Report number NREL-SR-580–24089, National Renewable Energy Laboratory, Golden, CO, 1998; pp 206–261.

(6) A comprehensive analysis of biodiesel impacts on exhaust emissions. Draft Technical Report number EPA420-P-02-001, U. S. Environmental Protection Agency, Washington, D.C., October, 2002.

(7) Westbrook, S. R. *Significance of Tests for Petroleum Products*, 7th ed.; Rand, S. J., Ed.; ASTM International: West Conshohocken, PA, 2003; pp 63–81.

(8) Giles, H. N. *Significance of Tests for Petroleum Products*, 7th ed.; Rand, S. J., Ed.; ASTM International: West Conshohocken, PA, 2003; pp 108–118.

10.1021/ef700412c
Published on Web 12/21/2007

and fuel lines, or microbial contamination from the migration of bacterial fungi on dust particles or within water droplets.[7,8] The present work emphasizes the thermo-oxidative component of biodiesel storage stability.

Biodiesel is a mixture of fatty acid monoalkyl esters with relatively high concentrations of long-chain mono- and polyunsaturated compounds to promote better cold flow properties. For example, methyl esters from soybean oil (SME) are typically composed of mostly fatty acid groups with 16- and 18-carbon chain lengths, where 80–85 wt % of the total mixture is unsaturated FAME.[9] These relatively high concentrations of mono- and polyunsaturated compounds make SME highly susceptible to oxidation.[10]

Maintaining and monitoring the fuel quality of biodiesel and its blends during storage presents a concern among fuel producers, suppliers, and users.[11,12] Adaptation of existing American Society of Testing and Materials (ASTM) method D 2274 (Oxidation Stability of Distillate Fuel—Accelerated Method) for application to biodiesel was viewed as unsuitable because of the formation of difficult to isolate soluble polymers during oxidation[13] and because attempts to correlate results with those from standard vegetable oils and fats industry methods to characterize oxidation were frustrated.[14] Although results from ASTM method D 4625 (Diesel Fuel Storage Stability at 43 °C) correlated well with field tests, the relatively long test periods associated with this method (4–16 weeks) eliminate it as a means to monitor or spot-check fuel stability during storage.[14–16] ASTM method D 5304 (Assessing Distillate Fuel by Oxygen Overpressure), an accelerated test for fuel stability,[7,8] may not be suitable because fatty derivatives tend to absorb oxygen or exhibit very broad decreases in pressure with time.[16,17]

Standard methods used by the vegetable oils and fats industry emphasize the isothermal measurement of an induction period whose termination is defined by the detection of secondary decomposition products. American Oil Chemists' Society (AOCS) method Cd 12b-92 [Oil Stability Index (OSI)] is an automated method for measuring the induction period using either the oxidative stability or Rancimat instruments.[18] An extensive collaborative study by Jebe et al.[19] showed that analysis of OSI by an oxidative stability instrument had lower interlaboratory coefficients of variation than those for OSI by the Rancimat instrument for hydrogenated and nonhydrogenated vegetable oils, margarines, and free fatty acids analyzed at 110 and 130 °C. The difference in coefficients of variation was attributed to higher variations in T for the Rancimat instrument.

The BIOSTAB project in Europe helped establish a unified test method (EN 14214) for biodiesel fuel stability based on analyses by the Rancimat instrument at 110 °C.[20,21] Lacoste and Lagardere[22] reported a good correlation between OSI and effects of oxidation on the acid value, kinematic viscosity, ester content, and linoleic acid content. Mittelbach and Schober[23] studied the oxidation of methyl esters derived from rapeseed, sunflower seed, used cooking oils, and tallow and demonstrated the utility of OSI for screening antioxidants. Bondioli et al.[15] showed that OSI may be used to monitor the degradation of biodiesel samples aged under storage conditions simulating ASTM method D 4625. Canakci et al.[13] observed that conducting OSI analyses at 110 °C was not suitable for evaluating high-iodine value biodiesel because of very rapid degradation. That study concluded that biodiesel derived from high-iodine value feedstocks should be analyzed at a maximum of 60 °C. Earlier studies on OSI analyses by an oxidative stability instrument resulted in the same general recommendation for the analysis of SME not treated by synthetic antioxidants or blended with petroleum middle distillates.[24,25]

The present work is a more detailed investigation on the effects of temperature on the OSI of biodiesel analyzed by an oxidative stability instrument. SME, using cooking oil FAME (UCOME) and pure methyl oleate (MO) as a reference standard, were analyzed isothermally at $T = 60$–95 °C in 5 °C increments. Two mathematical models were applied to results to determine how OSI varies with respect to temperature. The second model, ln(OSI) versus T^{-1}, was interpreted to determine the activation energy (E_a) for the first-order oxidation of FAME.

Experimental Section

Materials. Nexsol (SME) from Peter Cremer (Cincinnati, OH) was obtained through Procter and Gamble Chemical (Cincinnati, OH). Gas chromatographic (GC) analysis revealed a fatty acid composition of 12.3 wt % palmitic, 4.1% stearic, 23.6% oleic, 53.5% linoleic, and 6.5% linolenic acids for SME. Used cooking oil biodiesel (UCOME) was obtained directly from Griffin Industries (Chicago, IL). GC analysis revealed a fatty acid composition of 0.6% myristic, 15.7% palmitic, 0.9% palmitoleic, 7.8% stearic, 45.8% oleic isomers (7.5% *trans*), 24.4% linoleic (1.4% *trans*), and 2.0% linolenic acids plus a trace (<0.05%) of lauric acid and 2.9% unidentified. Fuel characteristics of SME and UCOME are summarized in Table 1. MO (>99 wt % 9*Z*-octadecenoic acid methyl ester) was used as received from Nu Chek Prep (Elysian, MN) and carefully stored after opening. None of the FAME samples were treated with antioxidants after acquisition.

Methods. Before analysis by an oxidative stability instrument, samples were vacuum-distilled to remove volatile contaminants that could interfere with analysis. Distillation was conducted under 0.05–0.10 mmHg absolute pressure at 60 °C for 90 min in a Kugelrohr apparatus from Aldrich (Milwaukee, WI).

Analyses of OSI were conducted according to AOCS method Cd 12b-92,[18] with an oxidative stability instrument from Omnion, Inc. (Rockland, MS). A 5 g sample was placed in a glass test tube held stationary within a thermostat-controlled (±0.1 °C) block heater. The test tube was capped with a two-hole rubber stopper to allow for a steady stream of clean dry air to pass through the sample

(9) Knothe, G.; Van Gerpen, J. H.; Krahl, J. *The Biodiesel Handbook*; AOCS Press: Champaign, IL, 2005; p 281.
(10) Gunstone, F. D. *Inform* **1995**, *6*, 1165–1169.
(11) Kearny, T.; Benton, J., Final Report. Air Force Biodiesel Demonstration Program at Scott Air Force Base, Scott Air Force Base, IL, 2002.
(12) Stavinoha, L. L.; Howell, S. *SAE Special Publication SP-1482: Alternative Fuels*; Society of Automotive Engineers: Warrendale, PA, 1999; pp 79–83.
(13) Canakci, M.; Monyem, A.; Van Gerpen, J. H. *Trans. ASAE* **1999**, *42*, 1565–1572.
(14) Monyem, A.; Canakci, M.; Van Gerpen, J. H. *Appl. Eng. Agric.* **2000**, *16*, 373–378.
(15) Bondioli, P.; Gasparoli, A.; Bella, L. D.; Tagliabue, S. *Eur. J. Lipid Sci. Technol.* **2002**, *104*, 777–784.
(16) Stavinoha, L. L.; Howell, S. Biodiesel Stability Test Methods. Proceedings: IASH 2000: The 7th International Conference on Stability and Handling of Liquid Fuels, Graz, Austria, September, 2000.
(17) Hassel, R. L. *J. Am. Oil Chem. Soc.* **1976**, *53*, 179–181.
(18) *Official Methods and Recommended Practices of the AOCS*, 5th ed.; Firestone, D., Ed.; AOCS Press: Champaign, IL, 1999; method Cd 12b-92.
(19) Jebe, T. A.; Matlock, M. G.; Sleeter, R. T. *J. Am. Oil Chem. Soc.* **1993**, *70*, 1055–1061.
(20) *Automotive Fuels—Fatty Acid Methyl Esters (FAME) for Diesel Engines—Requirements and Test Methods*. European Committee for Standardization (CEN): Brussels, Belgium, 2002; method prEN 14214.
(21) Prankl, H. *Eur. J. Lipid Sci. Technol.* **2002**, *104*, 371–375.
(22) Lacoste, F.; Lagardere, L. *Eur. J. Lipid Sci. Technol.* **2003**, *105*, 145–155.
(23) Mittelbach, M.; Schober, S. *J. Am. Oil Chem. Soc.* **2003**, *80*, 817–823.
(24) Dunn, R. O. *J. Am. Oil Chem. Soc.* **2005**, *82*, 381–387.
(25) Dunn, R. O.; Knothe, G. *J. Am. Oil Chem. Soc.* **2003**, *80*, 1047–1048.

Table 1. Fuel-Related Properties of Soybean Oil FAME (SME) and Used Cooking Oil FAME (UCOME)[a]

property	SME	UCOME
acid value (mg of KOH/g)	0.18 ± 0.021	0.60 ± 0.016
kinematic viscosity at 40 °C (mm^2/s)	4.424 ± 0.0073	4.861 ± 0.0068
specific gravity at 15.6 °C	0.891 ± 0.0021	0.8839 ± 0.00059
cloud point (°C)	−0.1 ± 0.35	7.0 ± 0.31
free glycerin (% mass)	0.050	<0.02
total glycerin (% mass)	<0.13	<0.18
iodine value (g of I_2/100 g)	129.4	87.3

[a] FAME = fatty acid methyl esters; SME (Nexsol) from Peter Cremer and UCOME from Griffin Industries.

and out the tube. Effluent air containing vaporized products (organic acids) was subsequently swept into a second vessel containing deionized water. Conductivity of the deionized water was monitored and recorded automatically every 3 min by a desktop personal computer programmed with data acquisition/control/analysis software from Omnion, Inc. OSI is defined as the induction period or oxidation onset time and was automatically determined by software analysis. This value was calculated as the maximum change in the rate of oxidation defined by the maximum of the second derivative of the conductivity versus the time curve. OSI data were obtained by averaging results from three replicate analyses of samples at each *T*. *T* was increased in 5 °C intervals in the range of 60–80 °C for SME, 70–95 °C for UCOME, and 60–95 °C for MO.

Acid value, kinematic viscosity, cloud point, and free and total glycerin were determined using an apparatus and procedures specified in ASTM methods D 664, D 445, D 5773, and D 6584.[26–29] Specific gravities were determined using AOCS method Cc 10–95.[30] GC analyses of FAME samples were conducted on a Varian model 3400 GC fitted with a 30 m × 25 mm i.d. SP-2330 column and flame ionization detector (FID; Palo Alto, CA). The carrier gas was helium. For analysis of fatty acid compositions, the temperature program was (1) held at 150 °C for 15 min, (2) ramped at 2°/min to 210 °C, (3) ramped at 50°/min to 220 °C, and (4) held at 220 °C for 5 min. Temperature programming for the analysis of free and total glycerin was as specified in ASTM method D 6584.[29]

Results and Discussion

Table 2 is a summary of OSI data obtained from the analysis of SME, UCOME, and MO with respect to temperature ranges outlined in the previous section. Also summarized are response factors (RF) for SME and UCOME calculated by the following equation:

$$\mathrm{RF} = (\mathrm{OSI\ of\ FAME})/(\mathrm{OSI\ of\ MO}) \quad (1)$$

where OSI data are taken at the same *T*.

Increasing *T* accelerates the oxidation reaction, resulting in a decrease in OSI for SME, UCOME, and MO. Although RF values decreased slightly with an increasing *T*, under conditions of the present work, these values were nearly constant at 0.041 ± 0.0075 for SME and 1.6 ± 0.20 for UCOME. This suggests that the oxidation reaction pathways for SME and UCOME were similar to those for MO over corresponding *T* ranges. Furthermore, reaction pathways for SME and UCOME each do not vary significantly as *T* increased over the corresponding ranges studied in this work.

Table 2. OSI and RF Data from the Analysis of FAME by an Oxidative Stability Instrument[a]

	SME		UCOME		MO
T (°C)	OSI (h)	RF	OSI (h)	RF	OSI (h)
60	6.2	0.0437			141
65	4.4	0.048			92
70	2.1	0.042			51
75	1.25	0.028	81	1.8	45
80	1.1	0.042	48	1.8	27
85			29.2	1.6	18
90			17.9	1.4	13
95			11	1.4	7.7

[a] Variances: 0.0050−0.22 for SME, 0.18–4.5 for UCOME, and 0.65−41 for MO. *T* = block temperature; MO = methyl oleate (>99 wt % 9*Z*-octadecenoic acid methyl ester); OSI = oil stability index; RF = response factor = (OSI of FAME)/(OSI of MO) at the same *T*. See Table 1 for abbreviations.

A comparison of OSI data of SME and MO was consistent with respect to their iodine values. That is, SME has a much higher iodine value (129.4) than MO (85.6);[31] hence, SME had a significantly lower OSI than MO. In contrast, the iodine value of UCOME (87.3) is nearly equivalent to that of MO, yet UCOME had higher OSI values across the *T* range studied. The most likely explanation for the contrast in results is the possible presence of antioxidants in UCOME as received for the present study compared to zero antioxidant content in the pure MO.

Results in Table 2 may be explained by comparing the fatty acid compositions with respect to di- and trienic hydrocarbon chains present in FAME. Iodine value accounts only for the total number of double bonds present in the oil relative to the molecular weight. Oxidation of fatty derivatives generally proceeds at rates depending upon the position of double bonds as well as their total number.[32] The allylic positions (methylene positions adjacent to a double bond) are especially susceptible to oxidation. Furthermore, polyunsaturated fatty acid chains with bis-allylic methylene positions (for example, linoleic acid has one bis-allylic position at C-11 between double bonds at Δ9 and Δ12) are more prone to oxidation than allylic positions. The relative rate of the oxidation reaction of linolenate/linoleate/oleate (methyl and ethyl esters) was reported to be 98:41:1.[32] An earlier study[33] showed that OSI of various FAME correlates better with respect to bis-allylic position equivalents than the iodine value.

When data in Table 2 were compared again, SME had much higher C18:2 and C18:3 contents (53.5 and 6.5 wt %) than either UCOME (24.4 and 2.0 wt %) or MO (zero). An application of equations reported by Knothe[31] for SME yielded a bis-allylic position equivalent (BAPE) = 66.5 compared to BAPE = 28.4 for UCOME and 0 for MO. Given its higher BAPE value, SME is substantially more susceptible to oxidation and has a significantly lower OSI than UCOME or MO (at 75 and 80 °C).

A direct comparison of fatty acid compositions for UCOME and MO is more problematic. First, UCOME did not have a relatively high total saturated FAME content (24.1 wt %) in the present study. Again, an application of equations reported by Knothe[31] of allylic position equivalents (APE) for UCOME and MO was 146.2 and 200, respectively, suggesting a higher stability for UCOME with respect to oxidation. However, as

(26) *Annual Book of ASTM Standards*; ASTM International: West Conshohocken, PA, 2003; Vol. 05.01, ASTM method D 445.
(27) *Annual Book of ASTM Standards*; ASTM International: West Conshohocken, PA, 2003; Vol. 05.01, method D 664.
(28) *Annual Book of ASTM Standards*; ASTM International: West Conshohocken, PA, 2003; Vol. 05.03, ASTM method D 5773.
(29) *Annual Book of ASTM Standards*; ASTM International: West Conshohocken, PA, 2003; Vol. *05.04*, method D 6584.
(30) *Official Methods and Recommended Practices of the AOCS*, 5th ed.; Firestone, D., Ed.; AOCS Press: Champaign, IL, 1999; method Cc 10-95.
(31) Knothe, G. *J. Am. Oil Chem. Soc.* **2002**, *79*, 847–854.
(32) Frankel, E. N. *Lipid Oxidation*, 2nd ed.; The Oily Press: Bridgewater, U.K., 2005; pp 15–22.
(33) Knothe, G.; Dunn, R. O. *J. Am. Oil Chem. Soc.* **2003**, *80*, 1021–1026.

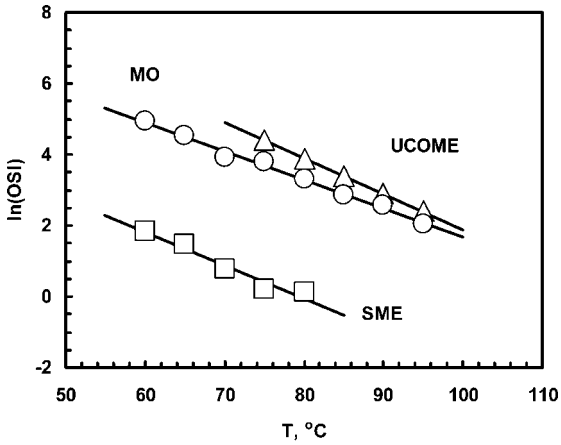

Figure 1. Results plotted according to model A, ln(OSI) versus T. OSI = oil stability index; T = block temperature; SME = soybean oil fatty acid methyl ester (FAME); UCOME = used cooking oil FAME; MO = methyl oleate (+99%).

noted above, UCOME has a significantly higher BAPE value than MO. Because bis-allylic methylene positions are approximately 2.5 times more reactive to oxidation than allylic positions, it is difficult to suggest that the lower APE value overrides a higher BAPE value in determining the OSI of UCOME with respect to pure MO. Thus, the possible presence of antioxidants in UCOME remains the most likely explanation for the UCOME, yielding substantially higher OSI values with respect to MO, despite their nearly equivalent iodine values.

The aforementioned similarities between reaction pathways for FAME studied in the present work suggested that OSI$-T$ data may be mathematically modeled. The following two equations were examined:

$$\text{Model A:}\quad \ln(\text{OSI}) = A_0 + A_1(T) \tag{2}$$

where T is in °C and A_0 and A_1 are constants, and

$$\text{Model B:}\quad \ln(\text{OSI}) = B_0 + B_1(T^{-1}) \tag{3}$$

where T is the absolute temperature in K and B_0 and B_1 are constants. Results from the application of these models are discussed separately below.

Model A. Nakatani et al.[34] showed that plotting log(OSI) versus T according to eq 2 yields a linear relationship for blends of 95% methyl linoleate in silicone oil. Similar results were reported from studies of various oils by Jebe et al.,[19] Hassenhuettl and Wan,[35] Mendez et al.,[36] and Reynhout.[37]

Figure 1 is a graph of ln(OSI) versus T curves for SME, UCOME, and MO studied herein. Results from least-squares linear regression of these curves are summarized in part a of Table 3. The regression results show a linear correlation (coefficients of deviation, $R^2 > 0.99$) with respect to UCOME and MO. Although SME exhibits near-linear correlation, $R^2 = 0.94$ was low mainly because of the scatter in the data.

Results for SME in Figure 1 compared well to those from an earlier study,[25] where regression analysis of ln(OSI) versus T curves for neat SME yielded intercept = 6.7 and slope = −0.079. Although slopes (A_1) of all three FAME were similar in the range from −0.081 to −0.0999, intercepts (A_0) were very

Table 3. Results from the Regression Analysis of OSI and T Data Shown in Table 2 with Respect to Models A and B[a]

(a) Model A: $\ln(\text{OSI}) = A_0 + A_1(T)$, where T is in °C

FAME	n	A_0	A_1	R^2	σ_y
SME	5	7.4 ± 0.82	−0.09 ± 0.012	0.94	0.18
UCOME	5	11.87 ± 0.062	−0.0999 ± 0.00073	0.9998	0.012
MO	8	9.7 ± 0.22	−0.081 ± 0.0028	0.992	0.091

(b) Model B: $\ln(\text{OSI}) = B_0 + B_1(T^{-1})$, where T is in K

FAME	n	B_0	B_1	R^2	σ_y
SME	5	−31 ± 3.8	11000 ± 1300	0.94	0.18
UCOME	5	−32.4 ± 0.13	12800 ± 46	0.99995	0.0057
MO	8	−25 ± 1.0	9900 ± 360	0.991	0.095

[a] n = total number of data points analyzed; A_0 and B_0 = intercepts; A_1 and B_1 = slope; R^2 = coefficient of deviation adjusted for degrees of freedom; σ_y = standard error of the y estimate. See Tables 1 and 2 for abbreviations.

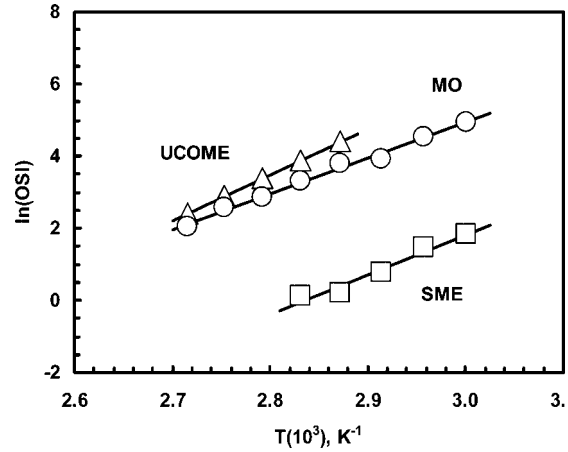

Figure 2. Results plotted according to model B, ln(OSI) versus T^{-1}. See Figure 1 for other abbreviations.

dissimilar. Nakatani et al.[34] reported a slope = −0.069 from studies on methyl linoleate and its blends in silicone oil. Jebe et al.[19] reported a slope = −0.07 for soybean oil, and Mendez et al.[36] reported a slope = −0.07 for fish oils.

The results in Table 3a show statistically significant ($p < 0.001$) deviation between A_1 data for UCOME and MO. In contrast, a similar comparison demonstrated a small probability (0.36) favoring equivalent A_1 values between SME and MO. It is known that the presence of antioxidants in fatty derivatives cause the slope of Arrhenius plots, such as Figure 1, to decrease relative to uninhibited derivatives.[38] Hence, results in Table 3a also suggest that antioxidants were present in UCOME before its acquisition. With respect to A_0 results, the data in Table 3a show substantial variations for SME, UCOME, and MO most likely because of the substantial differences in fatty acid composition between these three FAME.

Model B. The early stages of oxidation typically follow first-order reaction kinetics.[32,39–41] If this is the case for the analysis of FAME oxidation by OSI, then a plot of ln(OSI) versus T^{-1} should yield a straight line with a positive slope, such as that described in eq 3. Figure 2 is a graph of ln(OSI)$-T^{-1}$ curves

(34) Nakatani, N.; Tachibana, Y.; Kikuzaki, H. *J. Am. Oil Chem. Soc.* **2001**, *78*, 19–23.
(35) Hassenhuettl, G. L.; Wan, P. J. *J. Am. Oil Chem. Soc.* **1992**, *69*, 525–527.
(36) Mendez, E.; Sanhueza, J.; Speisky, H.; Valenzuela, A. *J. Am. Oil Chem. Soc.* **1996**, *73*, 1033–1037.
(37) Reynhout, G. *J. Am. Oil Chem. Soc.* **1991**, *68*, 983–984.
(38) Frankel, E. N. *Lipid Oxidation*, 2nd ed.; The Oily Press: Bridgewater, U.K., 2005; pp 165–170.
(39) Litwinienko, G.; Daniluk, A.; Kasprzycka-Guttman, T. *Ind. Eng. Chem. Res.* **2000**, *39*, 7–12.
(40) Blaine, S.; Savage, P. E. *Ind. Eng. Chem. Res.* **1992**, *31*, 69–75.
(41) Garcia-Ochoa, F.; Romero, A.; Querol, J. *Ind. Eng. Chem. Res.* **1989**, *28*, 43–48.

Table 4. Activation Energies (E_a) Calculated from the Slope of Model B Curves Shown in Figure 2[a]

FAME	E_a (kJ/mol)	ζ/Z ratio
SME	90 ± 11	3.30×10^{-14}
UCOME	106.4 ± 380	8.75×10^{-15}
MO	82 ± 3.0	1.87×10^{-11}

[a] $\zeta = -\ln(1 - \alpha)$, where α is the degree of conversion at OSI; Z = Arrhenius pre-exponential factor for the reaction constant. See Tables 1 and 2 for abbreviations.

for SME, UCOME, and MO data (from Table 2). Results from a least-squares linear regression of these curves summarized in Table 3b confirm the linear behavior ($R^2 > 0.99$) for UCOME and MO and nearly linear behavior ($R^2 = 0.94$) for SME.

In addition to providing a correlation for estimating OSI as a function of T, modeling according to model B provides a means for quantifying kinetic parameters for the oxidation reaction. For first-order reaction kinetics, the rate of increasing the degree of conversion (α) may be expressed by the following equation:

$$d\alpha/dt = k(1 - \alpha) \quad (4)$$

where t is the reaction time and k is the reaction coefficient. Rearranging and integrating from t_0 to t^* and from 0 to α*, where t^* and α* are defined by the induction period for oxidation (OSI), yields the following:

$$\text{OSI} = \zeta/k \quad (5)$$

where $\text{OSI} = \Delta t = (t^* - t_0)$ and ζ is defined as follows:

$$\zeta = -\ln(1 - \alpha^*) \quad (6)$$

For a given FAME, α* is constant at all temperatures where OSI is analyzed; hence, ζ is also constant.

The rate of the oxidation reaction (eq 4) is exponentially related to temperature.[38] Consequently, k is dependent upon T and generally expressed by the Arrhenius relation

$$k = Z[e^{-E_a/R_gT}] \quad (7)$$

where Z is the frequency factor, E_a is the reaction activation energy, and R_g is the gas constant. Substituting eqs 6 and 7 into eq 5 and taking the natural log of the resulting equation yields the following:

$$\ln(\text{OSI}) = \ln(\zeta/Z) + (E_a/R_g)T^{-1} \quad (8)$$

A comparison of eq 8 with model B as expressed in eq 3 leads to the following expressions:

$$B_0 = \ln(\zeta/Z) \Rightarrow \zeta/Z = e^{B_0} \quad (9)$$

$$B_1 = (E_a/R_g) \Rightarrow E_a = R_gB_1 \quad (10)$$

For first-order oxidation reactions, regression coefficients summarized in Table 3b may be used in eqs 9 and 10 to determine the "ζ/Z" ratio and E_a associated with a FAME mixture. Corresponding results for SME, UCOME, and MO are summarized in Table 4. Litwinienko[42] studied kinetics of oxidation of fatty acids and esters by isothermal differential scanning calorimetry and reported $E_a = 85.5$ kJ/mol for ethyl oleate, a compound very similar to MO. That value that compared well to $E_a = 82 \pm 3$ kJ/mol for MO is shown in Table 4.

The pre-exponential factor Z may only be calculated from eq 9 when α* at OSI is known. A precise evaluation of α from the oxidation of complex FAME mixtures was beyond the scope of the present study. A comprehensive study on rates of conversion during the oxidation of FAME under conditions simulating OSI analyses should be performed in the future.

(42) Litwinienko, G. *J. Therm. Anal. Calorim.* **2001**, *65*, 639–646.

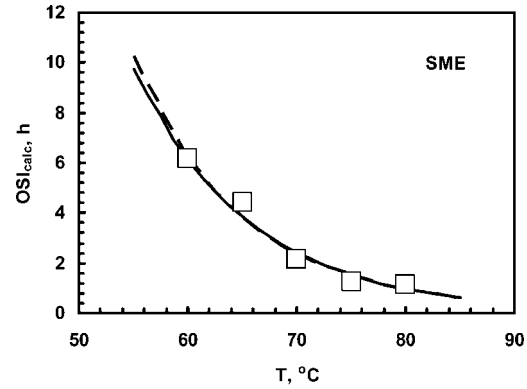

Figure 3. Calculated OSI (OSI_{calc}) of SME as a function of temperature (T) predicted by models A (—) and B (- - -). Data points are measured OSI values from Table 2. See Figure 1 for other abbreviations.

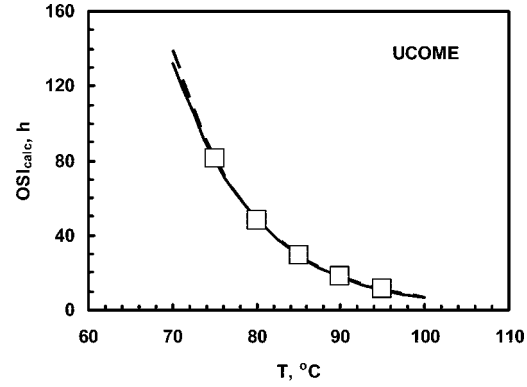

Figure 4. OSI_{calc} of UCOME as a function of T predicted by models A (—) and B (- - -). Data points are measured OSI values from Table 2. See Figures 1 and 3 for other abbreviations.

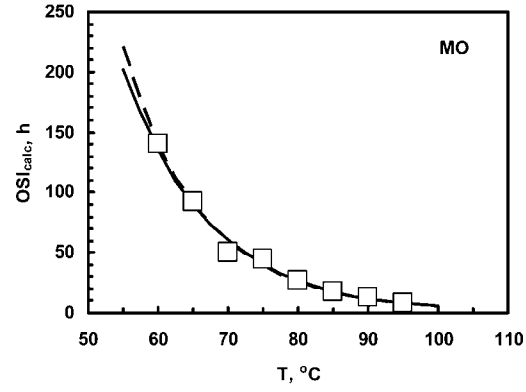

Figure 5. OSI_{calc} of MO as a function of T predicted by models A (—) and B (- - -). Data points are measured OSI values from Table 2. See Figures 1 and 3 for other abbreviations.

Calculated OSI. Regardless of whether α* may be accurately determined at $\Delta t = \text{OSI}$ or whether E_a or pre-exponential factor Z are precisely known for a given FAME, if regression coefficients are known, OSI may be calculated (OSI_{calc}) at a given temperature by directly applying eqs 2 or 3 outlined above. Figures 3−5 are graphs showing OSI_{calc} as a function of T for SME, UCOME, and MO from corresponding coefficients listed in Table 3. In comparison between both models, curves in Figures 3−5 show very good agreement at higher T, while model B predicts a slightly more rapid increase in OSI_{calc} at lower T.

Measured OSI data (Table 2) superimposed in Figures 3−5 demonstrated very good agreement with corresponding OSI_{calc}

curves. Calculated results may also be compared in terms of residuals (δ) determined as follows:

$$\delta = (\mathrm{OSI}_{\mathrm{calc}} - \mathrm{OSI}) \quad (11)$$

Application of eq 11 with $\mathrm{OSI}_{\mathrm{calc}}$ data from both models indicated a slight trend toward increasing δ with decreasing T. With respect to model A, maximum δ values were −0.57 h at 65 °C for SME, −0.94 h at 75 °C for UCOME, and 9.72 h at 70 °C for MO. With respect to model B, maximum δ values were −0.60 h at 65 °C for SME, 0.19 h at 75 °C for UCOME, and 8.60 h at 70 °C for MO.

Although maximum absolute δ values tended to increase with decreasing T, relative deviation as percent values behaved more erratically. SME demonstrated the 10–19% deviation with respect to $T \geq 65$ °C for both models; UCOME generally showed very small relative deviations (<1.2%) with respect to both models; and MO first increased and then decreased in relative deviation as T increased. Both the absolute and relative (%) deviations were generally smaller for model B than model A.

Linear relationships explored by models A and B may also be explored by extrapolation to estimate $\mathrm{OSI}_{\mathrm{calc}}$ at temperatures outside the analyzed T ranges in the present study. For example, models A and B yielded $\mathrm{OSI}_{\mathrm{calc}} = 15.5$ and 17.2 h for neat SME at 50 °C. These values compared well to measured OSI = 17.2 h reported in an earlier study.[25]

Extrapolation of $\mathrm{OSI}_{\mathrm{calc}}$ to reasonable storage temperatures was more problematic. At 30 °C, model A yields $\mathrm{OSI}_{\mathrm{calc}} = 99$ h for SME, 7180 h for UCOME, and 1520 h for MO. At the same temperature, model B yields $\mathrm{OSI}_{\mathrm{calc}} = 160$ h for SME, 19 100 h for UCOME, and 2650 h for MO. The results for SME appear to be an unrealistic estimation of the oxidation induction period at 30 °C. Furthermore, RF calculated as a ratio of $\mathrm{OSI}_{\mathrm{calc}}$ values for SME to MO (see eq 1) were 0.065 for model A and 0.060 for model B. These values were 50% higher at 30 °C than the RF value for the analyzed temperature range discussed earlier (Table 2). Similar increases were noted for RF ratios based on $\mathrm{OSI}_{\mathrm{calc}}$ of UCOME and MO at lower temperatures. Thus, it is apparent that calculating OSI from either model decreases in reliability as the temperature moves further away from the T range employed to develop the models. Nevertheless, results from the present study provide a means for determining effects of the temperature on OSI analyses of FAME under accelerated conditions relative to a reference standard, such as pure MO.

Conclusions

Increasing the temperature accelerated the oxidation reaction, which decreased OSI of the three FAME studied in the present work. RF values with respect to MO as a reference did not vary greatly for SME or UCOME over the corresponding T ranges studied. SME had a higher BAPE than MO, resulting in a significantly lower OSI at constant T. UCOME had a significantly higher OSI than MO, despite having a similar iodine value. The most likely explanation for this was the presence of antioxidants in UCOME before it was acquired for the present study.

The effects of T on OSI were examined by application of two models. Results from model A showed linear correlation between ln(OSI) and T and were in good agreement with those from similar studies published in the literature. Results from model B showed linear correlation between ln(OSI) and T^{-1}. This model was also used to calculate E_a data for the oxidation reaction based on first-order kinetics. E_a determined for MO in the present study agreed well with values for oleic acid ethyl esters in the literature.

Results from models A and B were used to calculate OSI values with respect to temperature. Model B predicted a slightly more rapid increase in $\mathrm{OSI}_{\mathrm{calc}}$ with decreasing T than model A. A comparison of $\mathrm{OSI}_{\mathrm{calc}}$ with measured OSI showed good agreement for all three FAME studied in the present work. Deviations between $\mathrm{OSI}_{\mathrm{calc}}$ and OSI showed no distinct pattern with respect T and were generally smaller for comparisons with model B. Extrapolation of results for SME at $T = 50$ °C yielded $\mathrm{OSI}_{\mathrm{calc}}$ that compared well to OSI data reported in an earlier study. However, application of both models demonstrated less reliability at temperatures below 50 °C.

Acknowledgment. Haifa Khoury, Kevin Steidley, and Kim Witt provided technical and analytical assistance for conducting this research. The mention of brand or firm names does not constitute an endorsement by the United States Department of Agriculture (USDA) over others of a similar nature not mentioned.

EF700412C